



The design of astigmatism-free crossed Czerny–Turner spectrometer

Yan An^{a,b}, Qiang Sun^a, Ying Liu^a, Chun Li^a, Zhao-Qi Wang^{c,*}

^a Opto-electronics Technology Center, Changchun Institute of Optics, Fine Mechanics and Physics, Changchun 130033, PR China

^b Graduate School of the Chinese Academy of Sciences, Beijing 100039, PR China

^c Key Laboratory of Opto-electronic Information Science and Technology, Ministry of Education, Institute of Modern Optics, Nankai University, Tianjin 300071, PR China

ARTICLE INFO

Article history:

Received 8 March 2012

Accepted 18 July 2012

Keywords:

Czerny–Turner
Crossed-structure
Astigmatism-free
Coma-free

ABSTRACT

The first-order astigmatism-free conditions in crossed Czerny–Turner (C–T) spectrometer are derived. To our best knowledge, there is no report about this kind of research. For the requirements of the optical parameters of the relative aperture of 8 and the working wavelength ranging from 780 nm to 1020 nm, according to the derived formula, the astigmatism-free crossed C–T spectrometer is built up with ZEMAX software. The correspondent coma-free crossed C–T spectrometer is also built up. The two initial structures of crossed C–T optical systems are then optimized, and the performance merits are compared. It is shown that, the astigmatism-free crossed C–T spectrometer has a superior optical performance, with the RMS of spot diagram only 12–52% that in the correspondent coma-free crossed C–T spectrometer. This indicates that the astigmatism-free crossed C–T spectrometer possesses not only a better energy concentration along the slit direction, which is beneficial to spectrometers requiring larger condenser capacity, but also a smaller spot diameter along the direction perpendicular to the slit, which implies a higher spectrum resolution achieved.

© 2012 Elsevier GmbH. All rights reserved.

1. Introduction

The Czerny–Turner (C–T) spectrometer satisfying the coma-free condition is one of the most commonly used mountings in micro-spectrometers. It possesses advantage of avoiding the secondary and multiple diffractions, usually existing in Ebert–Fastie spectrometer, by means of two mirrors separated. So it has wide applications in the detection of weak signals such as Raman spectrum [1] and in the detection of atmospheric remote sensing such as atmospheric limb imaging [2]. The original C–T spectrometer showed a symmetric arrangement with two off-axis mirrors oriented oppositely which can partially correct the aberrations. After that, Shafer showed that the coma can be corrected by unsymmetrical arrangement satisfying the condition of Shafer equation [3,4]. It could be no necessary to consider the impact of astigmatism in one-dimensional spectrometer with the photomultiplier tube as the detector. However, for the signal collection with high-speed linear CCD and CMOS, which are sensitive to energy, the astigmatism height at image plane caused by different focal lengths for tangential and sagittal beams is a fatal shortcoming. So extensive literature are reported trying to correct the astigmatism for classical C–T spectrometer, such as placing an additional convex mirror in front of the entrance slit [5], using toroidal

mirrors to compensate the astigmatism [6], placing an off-the-shelf cylindrical lens in front of the detector [7]. In particular, McDowell proposed the zeroth-order divergent illumination condition, valid for single wavelength, that the astigmatism of grating was used to compensate the astigmatism of two spherical mirrors [8]. After that, Austin further proposed the first-order divergent illumination condition to eliminate the astigmatism, valid for a wide spectrum band [9]. There is no additional optical component in Refs. [8,9] as compared with other techniques, and the astigmatism elimination is achieved by adjusting structure parameters.

For weak signal detection, the optical system with a strong condenser capacity is required. The condenser capacity of the classical C–T spectrometer is determined by the grating size that is restricted by the system miniaturization. In a comparison, the crossed C–T spectrometer has the advantage of stronger condenser capacity as well as lower stray light. The design of the crossed C–T spectrometer is usually under coma-free condition, which is with a quite large residual astigmatism.

In this paper, the first-order divergent illumination conditions to eliminate the astigmatism for the crossed C–T spectrometer are derived, and the calculation equations of the structure parameters are provided. Then a ray-tracing design of the optical system of the spectrometer of F/8 working in wavelength range of 780–1020 nm is presented, which is compared with its counterpart of coma-free crossed C–T spectrometer. To our best knowledge, there has been no this kind of research reported yet.

* Corresponding author.

E-mail address: wangzq@nankai.edu.cn (Z.-Q. Wang).

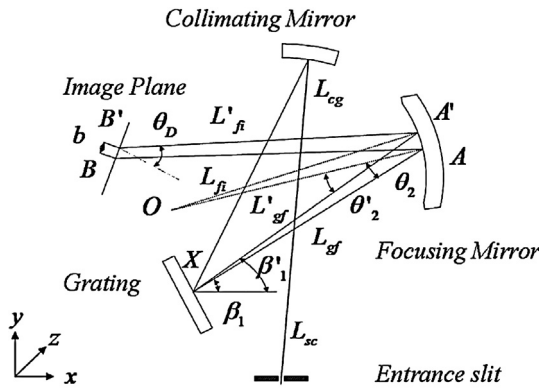


Fig. 1. The layout of crossed C-T spectrometer.

2. Divergent illumination conditions of crossed Czerny-Turner spectrometer

2.1. Zeroth-order divergent illumination condition

The zeroth-order divergent illumination condition for the correction of astigmatism of classical C-T spectrometer at single wavelength was proposed in Ref. [8]. The sagittal image distance S_S and the tangential image distance S_T can be expressed as:

$$S_T = \frac{R_1 R_2 S}{2S(R_1 \sec \theta_2 + R_2 \sec \theta_1 (\cos^2 \alpha / \cos^2 \beta) - R_1 R_2 (\cos^2 \alpha / \cos^2 \beta))} \quad (1)$$

$$S_S = \frac{R_1 R_2 S}{2S(R_1 \sec \theta_2 + R_2 \sec \theta_1) - R_1 R_2} \quad (2)$$

where S is the distance between the entrance slit and the collimating mirror, θ_1 and θ_2 are the incident angles of the collimating and the focusing mirror respectively, R_1 and R_2 are the radii of the collimating and the focusing mirror respectively, and α and β are the angles of the incidence and the diffraction of the grating respectively. With the condition of $S_T = S_S$ we have:

$$S = 0.5 \times \left[\frac{R_1 R_2 ((\cos^2 \alpha / \cos^2 \beta) - 1)}{R_1 (\sec \theta_2 - \cos \theta_2) + R_2 (\sec \theta_1 (\cos^2 \alpha / \cos^2 \beta) - \cos \theta_1)} \right] \quad (3)$$

Eq. (3) is also valid for the crossed C-T spectrometer, because the light propagation order in the two structures is the same: starting from the entrance slit, via the collimating mirror, the grating and the focusing mirror, and finally reaching the image plane.

2.2. First-order divergent illumination condition

For the crossed C-T spectrometer, we derive the first-order divergent illumination condition with the similar method as Ref. [9]. The optical configuration of the crossed C-T spectrometer is shown in Fig. 1, where L_{sc} is the distance of entrance slit to collimating mirror, L_{cg} is the distance of collimating mirror to grating, L_{gf} and L'_{gf} are the distances of grating to focusing mirror for central and adjacent rays respectively, L_{fi} and L'_{fi} are the distances of focusing mirror to image plane for central and adjacent rays respectively, β_1 and β'_1 are the angles forming by diffraction beam and horizontal line for central and adjacent rays respectively, θ_D is the tilted angle of image plane, b is the displacement on image plane between the central and adjacent rays, O is the center of focusing mirror, X is the intersection of incident ray on grating, A and A' are the intersections of the central and adjacent rays on focusing mirror respectively, and B and B' are the intersections of the central and adjacent rays on image plane respectively. The diffraction angle changes as wavelength, which makes the astigmatism varying as wavelength. It is the key point to make astigmatism independent of diffraction angle by adjusting the distances and angles mentioned above, which is

the first-order divergent illumination condition. The formula can be expressed as:

$$\frac{dS_T}{d\beta} = \frac{dS_S}{d\beta} = \frac{dL_{fi}}{d\beta} \quad (4)$$

It can be seen from Eqs. (1) and (2) that the tangential image distance S_T , the sagittal image distance S_S and the incident angle of focusing mirror θ_2 are related to diffraction angle, then we have:

$$\frac{dS_S}{d\beta_1} = \frac{\partial S_S}{\partial \theta_2} \frac{d\theta_2}{d\beta_1} \quad (5)$$

$$\frac{dS_T}{d\beta_1} = \frac{\partial S_T}{\partial \beta_1} + \frac{\partial S_T}{\partial \theta_2} \frac{d\theta_2}{d\beta_1} \quad (6)$$

Substituting Eqs. (5) and (6) into Eq. (4) we have:

$$\frac{d\theta_2}{d\beta_1} = \frac{\partial S_T / \partial \beta_1}{\partial S_S / \partial \theta_2 - \partial S_T / \partial \theta_2} \quad (7)$$

In order to get $d\theta_2/d\beta_1$ in crossed C-T spectrometer, we need to calculate the sum of the vectors around the path $\mathbf{XAOA'X'}$. According to Fig. 1, we establish the two dimensional vectors herein:

$$\mathbf{XA} = L_{gf}(\cos \beta_1, \sin \beta_1) \quad (8)$$

$$\mathbf{XA'} = L'_{gf}(\cos \beta'_1, \sin \beta'_1) \quad (9)$$

$$\mathbf{OA} = R_2[\cos(\beta_1 - \theta_2), \sin(\beta_1 - \theta_2)] \quad (10)$$

$$\mathbf{OA'} = R_2[\cos(\beta'_1 - \theta'_2), \sin(\beta'_1 - \theta'_2)] \quad (11)$$

$$\mathbf{AB} = L_{fi}[-\cos(\beta_1 - 2\theta_2), -\sin(\beta_1 - 2\theta_2)] \quad (12)$$

$$\mathbf{A'B'} = L'_{fi}[-\cos(\beta'_1 - 2\theta'_2), -\sin(\beta'_1 - 2\theta'_2)] \quad (13)$$

$$\mathbf{BB'} = b[\sin(\beta_1 - 2\theta_2 + \theta_D), -\cos(\beta_1 - 2\theta_2 + \theta_D)] \quad (14)$$

With the vector equation of $\mathbf{XA} + \mathbf{AO} + \mathbf{OA'} + \mathbf{A'X} = 0$, we get the following equations:

$$L_{gf} \cos \beta_1 - R_2 \cos(\beta_1 - \theta_2) + R_2 \cos(\beta'_1 - \theta'_2) - L'_{gf} \cos \beta'_1 = 0 \quad (15)$$

$$L_{gf} \sin \beta_1 - R_2 \sin(\beta_1 - \theta_2) + R_2 \sin(\beta'_1 - \theta'_2) - L'_{gf} \sin \beta'_1 = 0 \quad (16)$$

We differentiate Eqs. (15) and (16) with respect to β'_1 and then replace β'_1 with β_1 , we have:

$$\frac{dL_{gf}}{d\beta_1} = L_{gf} \tan \theta_2 \quad (17)$$

$$\frac{d\theta_2}{d\beta_1} = 1 - \frac{L_{gf}}{R_2 \cos \theta_2} \quad (18)$$

Similarly, with the vector equation of $\mathbf{OA} + \mathbf{AB} + \mathbf{BB'} + \mathbf{B'A'} + \mathbf{A'O} = 0$, we get the relationship between the distance from focusing mirror to image plane and the diffraction angle:

$$R_2 \cos(\beta_1 - \theta_2) - L_{fi} \cos(\beta_1 - 2\theta_2) + b \sin(\beta_1 - 2\theta_2 + \theta_D) + L'_{fi} \cos(\beta'_1 - 2\theta'_2) - R_2 \cos(\beta'_1 - \theta'_2) = 0 \quad (19)$$

$$R_2 \sin(\beta_1 - \theta_2) - L_{fi} \sin(\beta_1 - 2\theta_2) - b \cos(\beta_1 - 2\theta_2 + \theta_D) + L'_{fi} \sin(\beta'_1 - 2\theta'_2) - R_2 \sin(\beta'_1 - \theta'_2) = 0 \quad (20)$$

Again, we differentiate Eqs. (19) and (20) with respect to β'_1 , and then replace β'_1 with β_1 , we have:

$$\frac{db}{d\beta_1} = \sec \theta_D \left(L_{gf} - L_{fi} + \frac{2L_{gf}L_{fi}}{R_2 \cos \theta_2} \right) \quad (21)$$

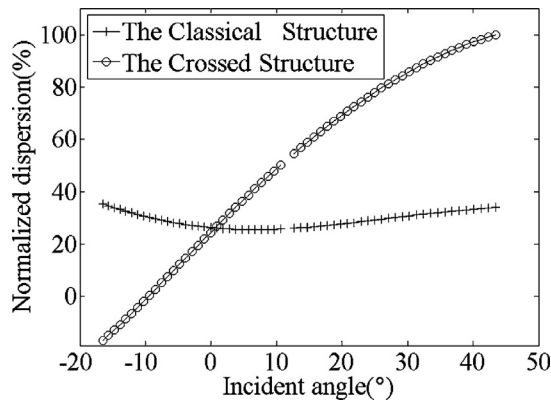


Fig. 2. Variations of the normalized linear dispersion as incident angle of grating for two types of C-T structures.

$$\frac{dL_{fi}}{d\beta_1} = \tan \theta_D \left(L_{fi} - L_{gf} - \frac{2L_{gf}L_{fi}}{R_2 \cos \theta_2} \right) + L_{gf} \tan \theta_2 \quad (22)$$

It can be seen in a comparison with Ref. [9] that Eqs. (17) and (18) are the same as that for classical C-T spectrometer, implying the distances between adjacent optical components in both structures are same. However, Eqs. (21) and (22) are different from that for classical C-T spectrometer, indicating that the linear dispersions and the tilted angle of image plane are different for both structures. The linear dispersion can be expressed as:

$$\frac{db}{d\lambda} = \frac{\partial \beta_1}{\partial \lambda} \frac{db}{d\beta_1} = \frac{m}{d \cos \beta_1} \frac{db}{d\beta_1} \quad (23)$$

where m is the diffraction order and d is groove spacing of the grating. With Eq. (23), the linear dispersions for two structures can be calculated, and the normalized linear dispersions as a function of incident angle of grating are shown in Fig. 2. Where the cross curve represents the normalized linear dispersion of classical C-T structure and the hollow circular curve represents that of crossed C-T structure. It can be seen that as the incident angle of grating varying from -16° to 44° , the linear dispersion of crossed C-T structure is in a range between 0% and 100%, while that of classical C-T structure is in a range between 25% and 45% which is more stable.

2.3. The structural solution

Firstly, with the common variable factor $d\theta_2/d\beta_1$, we solve the simultaneous equations of (7) and (18) to acquire the distance from grating to focusing mirror L_{gf} . The partial derivatives can be obtained from Eqs. (1) and (2):

$$\frac{\partial S_5}{\partial \theta_2} = \frac{2S_5L_{sc}R_1 \sin \theta_1}{2L_{sc}(R_1 \sec \theta_2 + R_2 \cos \theta_1) - R_1R_2} \quad (24)$$

$$\frac{\partial S_T}{\partial \beta} = \frac{-2S_T R_2 (2L_{sc} \sec \theta_1 - R_1) \cos^2 \alpha \tan \beta \sec^2 \beta}{2L_{sc}(R_1 \sec \theta_2 + R_2 \cos \theta_1 \cos^2 \alpha / \cos^2 \beta) - R_1R_2 \cos^2 \alpha / \cos^2 \beta} \quad (25)$$

$$\frac{\partial S_T}{\partial \theta_2} = \frac{-2S_T L_{sc} R_1 \sec \theta_2 \tan \theta_2}{2L_{sc}(R_1 \sec \theta_2 + R_2 \cos \theta_1 \cos^2 \alpha / \cos^2 \beta) - R_1R_2 \cos^2 \alpha / \cos^2 \beta} \quad (26)$$

Secondly, we use the zeroth-order divergent illumination condition of Eqs. (1)–(3) to determine the distance from entrance slit to collimating mirror L_{sc} and the distance from focusing mirror to image plane L_{fi} . Finally, we evaluate Eqs. (4) and (22) to determine the tilted angle of image plane θ_D . Since there is no constraint on L_{cg} , we set $L_{cg} = L_{sc} \times \cos \theta_1$ for convenience, and then we can determine all the anastigmatic parameters of crossed C-T spectrometer.

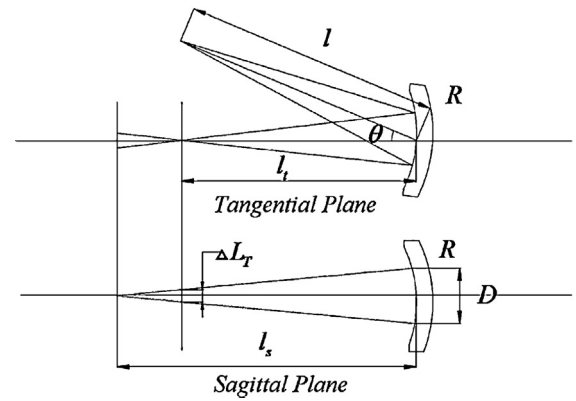


Fig. 3. The sagittal and tangential image distances of off-axis mirror.

3. The theoretical calculation of residual astigmatism

The first-order divergent illumination condition for the astigmatism-free crossed C-T structure guarantees astigmatism at center wavelength to be fully corrected and makes astigmatism in a certain range of wavelengths independent of the angle of diffraction. Therefore there still exists residual astigmatism blur at other wavelengths. Fig. 3 shows the sagittal and tangential imaging of an off-axis mirror with the object at finite distance, where R is the radius of the mirror, l is the object distance, θ is the incident angle of the mirror, l_t and l_s are the tangential and sagittal image distances respectively, D is the effective aperture of the mirror, and ΔL_T is the astigmatism blur height at tangential plane. It is clear from the geometric relationship of similar triangles that the astigmatism blur height can be calculated by:

$$\Delta L_T = \frac{l_s - l_t}{l_s} D \quad (27)$$

l_t and l_s can be obtained by following equations:

$$\frac{1}{l} + \frac{1}{l_t} = \frac{2}{R \cos \theta} \quad (28)$$

$$\frac{1}{l} + \frac{1}{l_s} = \frac{2 \cos \theta}{R} \quad (29)$$

Thus, as long as the effective aperture and the incident angle of the focusing mirror of the spectrometer are given, the residual astigmatism blur height at any wavelength can be calculated.

4. The comparison of structures and results of optimization

4.1. The comparison of two structures

Considering the theoretical formulas in Section 2, under the conditions of the grating of groove spacing $d = 1/450$ lp/mm, wavelength range from 780 nm to 1020 nm, radius of 100 mm for collimating and focusing mirrors, and the relative aperture of 8, as listed in Table 1, we simulate the astigmatism-free crossed C-T structures as the incident angle of grating varying. It is shown that in a range of the incident angles of grating from -10° to 0° , a rational astigmatism-free crossed C-T structure can be formed.

Table 1
The design parameters of the optical system.

Wavelength range (nm)	780–1020
Central wavelength (nm)	898
Grating of groove spacing (lp/mm)	1/450
The radius of collimating mirror R_1 (mm)	100
The radius of focusing mirror R_2 (mm)	100
F-number	8

Table 2
The initial parameters of astigmatism-free crossed structure and coma-free crossed structure (unit mm).

	Astigmatism-free crossed structure	Coma-free crossed structure
$i(^{\circ})$	−3.86	−3.86
$\theta_1(^{\circ})$	8	8
$\theta_2(^{\circ})$	8	8
L_{sc}	43.5	50.0
L_{cg}	41.8	42.3
L_{gf}	39.6	42.3
L_{fi}	60.2	50.0

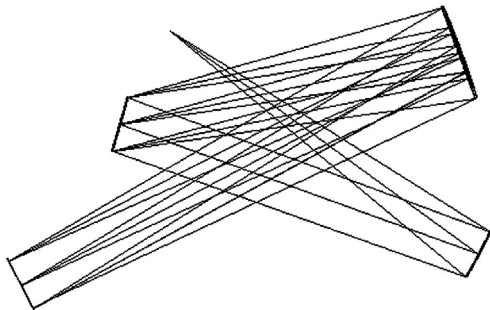


Fig. 4. The astigmatism-free crossed C-T spectrometer.

We set the incident angle of grating to be -3.86° , which is an angle to form a satisfactory symmetrical crossed C-T structure, and calculate the other parameters. The results are listed in Table 2. For comparison, we also form a coma-free crossed C-T structure with the same design parameters shown in Table 1, and calculate other initial parameters according to Ref. [10]. The results are also listed in Table 2. Figs. 4 and 5 show the layout of the astigmatism-free and the coma-free crossed C-T spectrometer respectively.

With simulation software, the specific effective apertures and the incident angles of the focusing mirror at any wavelength for each of the optical structures can be acquired. Then the astigmatism blur height is calculated according to formula (27) with the sample interval of wavelength of 10 nm. Fig. 6 shows the theoretical astigmatism blur height as a function of wavelength in two structures, where the cross curve represents the coma-free structure and the hollow circular curve represents the astigmatism-free structure. It can be seen from Fig. 6 that the astigmatism in the astigmatism-free crossed C-T structure does not completely eliminate overall. This is because the astigmatism-free design can eliminate the astigmatism only on the central wavelength and make the astigmatism in a certain range of wavelengths independent of the diffraction angle. As the wavelength increase or decreases from the central wavelength, the astigmatism blur height increases and forms a V-shaped curve. For the coma-free crossed C-T structure, there is residual

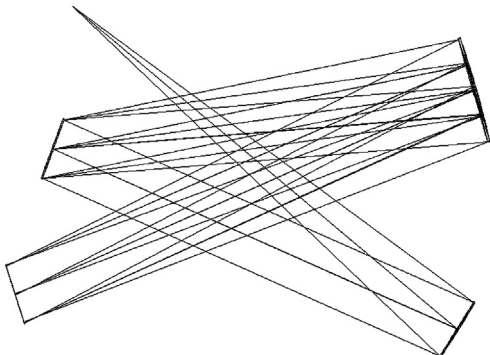


Fig. 5. The coma-free crossed C-T spectrometer.

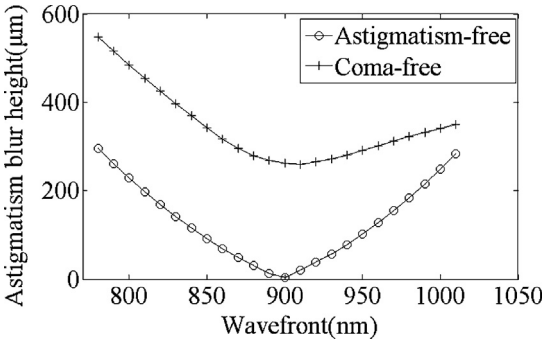


Fig. 6. The astigmatism blur height as a function of wavelength for two structures.

astigmatism blur height on the overall wavelength, which is much higher than that in the astigmatism-free C-T structure.

4.2. The practical optimization

ZEMAX is used to optimize the astigmatism-free and coma-free crossed C-T spectrometers, and the spot diagram is adopted to evaluate the performance of the two structures. Fig. 7 shows the spot diagram in the astigmatism-free crossed C-T spectrometer. It can be seen that the RMS is respectively 33.14 μm , 8.39 μm and 18.35 μm at wavelength of 780 nm, 898 nm and 1020 nm. Fig. 8 shows the spot diagram in the coma-free crossed C-T spectrometer. The RMS is respectively 55.89 μm , 44.39 μm and 35.57 μm at the three typical wavelengths. Fig. 9 shows the RMS value as a function of wavelength with the sampling interval of 10 nm. It can be seen

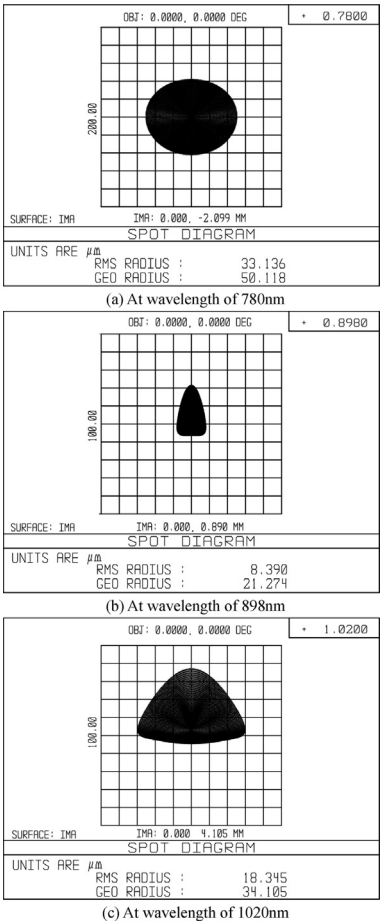


Fig. 7. Spot diagrams of astigmatism-free C-T structure at typical wavelengths.

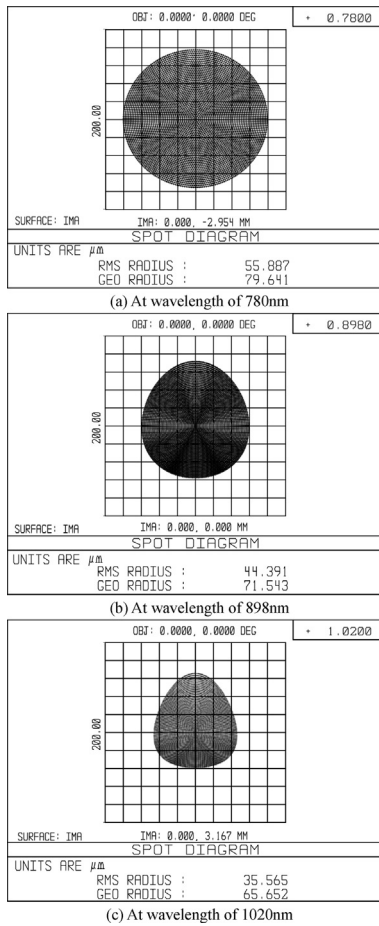


Fig. 8. Spot diagrams of coma-free C-T structure at typical wavelengths.

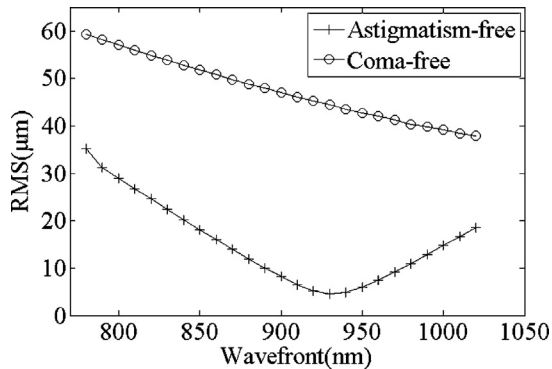


Fig. 9. The RMS of spot diagram of two optical systems after optimization.

in a comparison between Figs. 6 and 9, that the astigmatism blur height decreases dramatically by the optimization procedure. The maximum RMS value decreases from 300 μm to 36 μm in the wavelength range of 780–1020 nm for the astigmatism-free crossed C-T structure, and it is from 600 μm to 60 μm for the coma-free crossed C-T structure. The ratio of the RMS value of the spot diagram of the astigmatism-free crossed C-T structure to that of the coma-free crossed C-T structure is shown in Fig. 10. It can be seen that the RMS of the astigmatism-free crossed C-T structure is much smaller than that of the coma-free crossed C-T structure, with the smallest percentage of 12% and the largest percentage of 52% in the

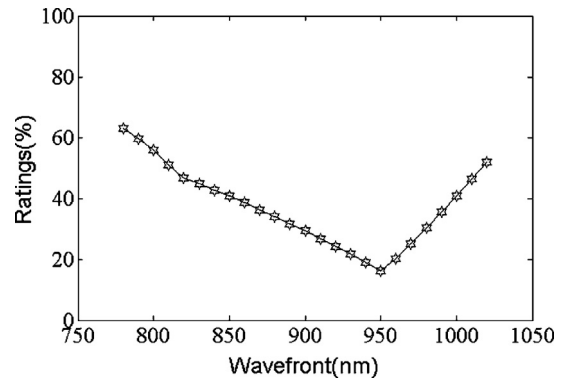


Fig. 10. The ratio of RMS of spot diagram between two structures.

working wavelength range. This result shows that the astigmatism-free crossed C-T spectrometer achieves a much higher spectral imaging resolution along the direction perpendicular to the slit and a much better energy concentration along the slit direction.

5. Summary and conclusions

We have derived the first-order astigmatism-free conditions in crossed C-T spectrometer, and designed the astigmatism-free crossed C-T spectrometer with the required optical parameters according to the derived formula. The correspondent coma-free crossed C-T spectrometer is also built up for a comparison. It is shown that the astigmatism-free crossed C-T spectrometer has a superior optical performance to the correspondent coma-free crossed C-T spectrometer, with the RMS of spot diagram being 12–52% in the whole wavelength range. This indicates that the astigmatism-free crossed C-T spectrometer possesses not only a better energy concentration along the slit direction, which is beneficial to spectrometers requiring larger condenser capacity, but also a higher spectrum resolution along the direction perpendicular to the slit.

Acknowledgments

This research is supported by the National Nature Science Foundation of China (No. 60977001), and the National High Technology Research and Development Program of China (No. 2007AA12Z110).

References

- [1] N. Hagen, D.J. Brady, Coded aperture DUV spectrometer for standoff Raman spectroscopy, *Proc. SPIE* 7319 (2009) 73190D–73191D.
- [2] Q.S. Xue, S.R. Wang, F.T. Li, L.G. Yu, L.Q. Wang, Limb imaging spectrometer for atmospheric remote sensing, *Opt. Prec. Eng.* 18 (4) (2010) 824–831.
- [3] A.B. Shafer, L.R. Megill, L. Droppleman, Optimization of the Czerny–Turner spectrometer, *J. Opt. Soc. Am.* 54 (7) (1964) 879–887.
- [4] A.B. Shafer, Correcting for astigmatism in the Czerny–Turner spectrometer and spectrograph, *Appl. Opt.* 6 (1) (1967) 159–160.
- [5] G.R. Rosendahl, Contributions to the optics of mirror systems and gratings with oblique incidence. III. Some applications, *J. Opt. Soc. Am.* 52 (4) (1962) 412–415.
- [6] Q.S. Xue, S.R. Wang, F.T. Li, Aberration-corrected Czerny–Turner imaging spectrometer with a wide spectral region, *Appl. Opt.* 48 (1) (2009) 11–16.
- [7] K.S. Lee, K.P. Thompson, J.P. Rolland, Broadband astigmatism-corrected Czerny–Turner spectrometer, *Opt. Express* 18 (22) (2010) 23378–23384.
- [8] M.W. McDowell, Design of Czerny–Turner spectrographs using divergent grating illumination, *Opt. Acta* 22 (1975) 473–475.
- [9] D.R. Austin, T. Witting, I.A. Walmsley, Broadband astigmatism-free Czerny–Turner imaging spectrometer using spherical mirrors, *Appl. Opt.* 48 (19) (2009) 3846–3853.
- [10] Z. Lin, S.F. Fan, *Spectroscopic Instrumentology*, Machine Industry Press, 1989.